

Abiotic crust formation in fallow agricultural desert soils through carbonate cementation reduces fugitive dust

Brian Scott¹, Jon Lima Zaloumis², Emmanuel Salifu³, Salim Alaufi³, Adesola Habeeb Adegoke³, Matthew Fraser⁴, Edward Kavazanjian³, Ferran Garcia-Pichel^{1,5*}

¹ Center for Fundamental and Applied Microbiomics, Biodesign Institute, Arizona State University, Tempe, Arizona, 85287, USA

² School of Earth and Space Exploration, Arizona State University, Tempe, Arizona, 85287-3005, USA

³ Center for Bio-mediated and Bio-inspired Geotechnics, School of Sustainable Engineering and the Built Environment, Arizona State University, Tempe, Arizona, 85287-3005, USA

⁴ School of Sustainable Engineering and the Built Environment, Arizona State University, Tempe, Arizona, 85287, USA

⁵ School of Life Sciences, Arizona State University, Tempe, Arizona, 85287-4501, USA

*** Corresponding author:**

Ferran Garcia-Pichel;

Email: ferran@asu.edu

This is an Open Access article, distributed under the terms of the Creative Commons Attribution-NonCommercial-NoDerivatives licence (<http://creativecommons.org/licenses/by-nc-nd/4.0/>), which permits non-commercial re-use, distribution, and reproduction in any medium, provided the original work is unaltered and is properly cited. The written permission of Cambridge University Press must be obtained for commercial re-use or in order to create a derivative work.

This peer-reviewed article has been accepted for publication but not yet copyedited or typeset, and so may be subject to change during the production process. The article is considered published and may be cited using its DOI.

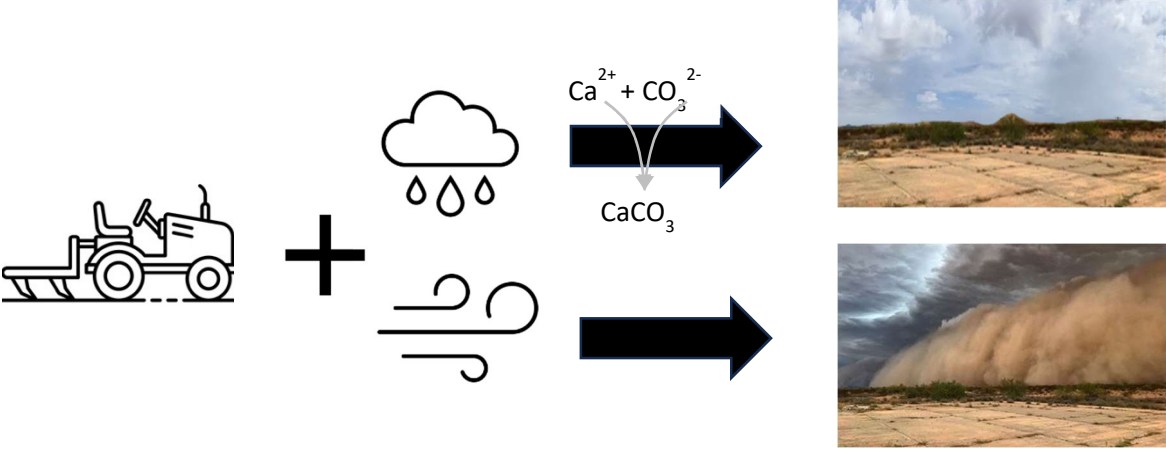
10.1017/dry.2024.5

Summary

Unconsolidated soils typically develop a physical surface crust after wetting and drying. We reproduced this process in the laboratory by wetting with fog and simulated rain on fallow agricultural soils from 26 locations, representing 15 soil types from Pinal County, Arizona. Through correlative analyses we found that carbonate content was a strong predictor of physical crust strength with fog ($p < 0.0001$, $R^2 = 0.48$) and rain ($p = 0.004$, $R^2 = 0.30$). Clay content increased crust strength ($p = 0.04$) but was not a useful predictor. Our results extend the current understanding of the soil crusting process, by highlighting the preeminence of carbonate cementation in desert soils. Consequently, we identify carbonate as a pragmatic tool for estimating crust strength, a surrogate measure of a soil's potential to produce fugitive dust, which can help prioritize interventions to curb airborne dust in arid lands.

Keywords: abiotic crust, fallow land, fugitive dust, dust storms, carbonates, management, mechanisms, resistance

Graphical Abstract



Impact Statement

Fugitive dust and dust storms are naturally occurring phenomena in arid and semi-arid environments (Ginoux et al. 2012). Airborne dust has a direct impact on human populations, leading to sometimes fatal traffic accidents (Henry et al. 2023; Joshi 2021), a variety of respiratory illnesses (Vergadi et al. 2022), and can serve as a vector for plant and animal pathogens (Finn et al. 2021). Human activities like vehicular traffic and plowing can increase dust generation and air particulate loads. Given the size of some dust storms, as large as 160 km in width and 2.4 km in height (Ramakrishnan et al. 2001), efforts to control them may seem futile. While soil stabilization technologies that prevent dust formation are available, their implementation at large scale is cost prohibitive (Heredia-Velásquez et al. 2023). Identification of soil stabilization targets where intervention would have a high impact would be very desirable. Our research suggests that carbonate content is a good predictor of how likely a soil is to become a significant fugitive dust source. It suggests that prioritizing the stabilization of soils low in carbonate, or strategically enhancing carbonate precipitation in them, could make interventions more effective.

Introduction

Global drylands are commonly characterized by elevated levels of airborne dust that cause a variety of environmental hazards (Middleton 2017). Dust production can be prevented or diminished by a variety of natural conditions. Vegetation provides a wind break and stabilizes surface soils against wind erosion (Tibke 1988; Vos et al. 2022). The soil surface itself may be inhabited by biological soil crusts that produce sticky, interwoven cellular material binding particles together (Belnap and Gillette 1997). Dryland soils may also form a variety of naturally occurring abiotic physical-chemical crusts that provide resistance against wind erosion (Williams et al. 2018).

The mechanisms of abiotic soil crusting have been widely studied, their mineral and chemical composition regarded to be the major inherent factor. The current consensus view is that abiotic crusts develop when plate-like clay particles become dispersed in water during rain events, migrating to soil surfaces, and, upon drying, align and stack horizontally, forming a surface seal (Awadhwai and Thierstein 1985; Williams et al. 2018). Clay dispersion is enhanced by Na^+ dissolution in low ionic strength rainwater (Forster and Goldberg 1990). Crusts formed by clay dispersion are termed depositional. Raindrops can amplify clay dispersion when their momentum is sufficient to break apart soil aggregates. Crusts formed under raindrop-induced dispersion are termed structural seals (Laker and Nortjé 2019). While clay minerals (e.g. montmorillonite, kaolinite and illite) vary in their crust-forming potential due to their differing dispersal behaviors (Forster and Goldberg 1990), it is difficult to generalize the role of a specific mineralogy on crust formation because constituent minerals differ markedly in their response to salts, pH, and organic matter (OM). Ca^{2+} (and other polyvalent cations, e.g. Mg^{2+}) generally stabilize soil by increasing flocculation and aggregate formation (Singer and Warrington 1992).

It is also acknowledged that Calcium (and magnesium) carbonate precipitation may also contribute to crusting through soil cementation (Williams et al. 2018). Carbonates are often a

mineral component of soils, particularly in arid and semi-arid environments, and can also act as binding agents increasing crust strength (Gillette et al. 1982). At extremely high carbonate contents, desert soils can form a true pavement (Bungartz et al. 2004). Interventional microbial or enzyme induced carbonate precipitation (MICP or EICP) for dust control (Hamdan and Kavazanjian 2016) is also based on carbonate cementation. A correlation between abiotic crusting potential has also been reported with potassium and pH (Stovall et al. 2022).

The presence of an abiotic crust increases the minimal wind velocities required to entrain soil particles in windflow (Vos et al. 2020) as well as their resistance to abrasion by saltating dust particles (Rice et al. 1996). But abiotic soil crusts can be disrupted by physical disturbance, such as is common in agricultural activity (Finn et al. 2021). Due to the large aerial footprint and ongoing disturbance, agricultural fields can be significant dust sources at the landscape scale (Ginoux et al. 2012; Joshi 2021; Li et al. 2018). In actively cultivated fields dust potential is temporary, as crops and irrigation offer some wind erosion resistance. Fallow fields are not irrigated, and weedy vegetation has to be removed, usually by plowing (Piemeisel et al. 1951). Plowing is also used for pest control and in some cases to break up hard soil pans in preparation for future cultivation, a practice known as “preparatory tillage” (Oswal 1994). Thus, while these practices serve useful purposes, they may render otherwise naturally stable soils into continuous and significant dust sources. Water scarcity and urbanization takes active dryland farms out of service, exacerbating atmospheric dust loads (Huang et al. 2017). Thus, fallow dryland agricultural fields act as a major, and increasing, source of atmospheric dust, with its associated environmental consequences.

We posit that a better mechanistic understanding of crust formation in drylands can be instrumental in predicting dust-forming potential of soils. Current models, based primarily on clay dispersion and stacking, are mechanistically accurate but do not provide a useful predictive tool. We investigated which, if any, soil compositional factors correlate to soil crust strength. Further, we hypothesized that a soil's carbonate content was most likely to predict abiotic crust formation

potential and crust strength. The role of carbonate is independent of mineralogy and raindrop momentum as it relies solely on dissolution (on wetting) and reprecipitation (on drying) at the soil-atmosphere interface (surface cementation). To test our hypothesis, we conducted a study of diverse fallow agricultural soils from Pinal County, Arizona with varying carbonate contents. We generated surface crusts using a wetting and drying cycles, with and without raindrop momentum, and measured crusts strength. Then we determined which compositional factors were best correlated with a soil's physical crust strength. Our findings shed light on the mechanisms of crust formation contributing to better predict which soils are likely dust sources. This, in turn, may help develop land management guidelines that promote abiotic crusting during fallow periods while still meeting the plowman's needs.

Methods

Sample Locations, sampling and sample preparation

Soil samples were collected from fallow agricultural fields with a variety of soil types in Pinal County, Arizona. Sample locations are shown in Figure 1. Soil types (series) were assigned by location based on the United States Department of Agriculture – National Cooperative Soil Survey (NCSS), accessible through the University of California (Davis) online browser (<https://casoilresource.lawr.ucdavis.edu/gmap/>). We selected and sampled 15 soil types to represent a range of relevant physical and chemical properties as listed in Table 1. The sample names are derived from the first three characters of the corresponding soil series name (e.g. Gladsen = Gla), except in the case of Casa Grande (= CG), which appears at two locations, identified with the numerals “3” and “4” on the NCSS map. Accordingly, these samples are identified as CG3 and CG4. In cases where we collected two or more samples within the same soil series name, we added a lower-case identifier [e.g., CG3(a) and CG3(f)].

We sampled the upper 5 cm of the soil, sieving samples through a 40 mesh (0.425 mm) screen to remove pre-formed peds, seeds, and very coarse sand, allowing for air drying prior to analysis. Residual soil moisture was determined by drying for 10 minutes in a microwave oven (Jalilian et al. 2017). In all cases initial soil moisture was < 6.7 %. We used the measured residual moisture content to correct gravimetrically determined soil weight.

Chemical, textural and structural characterization

The Schiebler volumetric method (ASTM D4373-21) was used to measure soil carbonate in triplicate using an Eijkelkamp Calcimeter. Dry soil specimens were treated with 4 M hydrochloric acid (HCl) to produce CO₂ gas from carbonates, which was quantified by water displacement. The method was calibrated using commercially obtained calcium carbonate powder. Although the method implies the CO₂ gas evolves from calcium carbonates, magnesium carbonates may also be detected, thus we specify these results broadly as “carbonate”. Standard geological thin sections (40 µm thick) were prepared from field crusted soils for microscopic examination using EpoFix epoxy resin (Tippkötter and Ritz 1996). Epoxy impregnation of the soils was achieved under vacuum and left to cure overnight. Polished thin sections were prepared commercially by Spectrum Petrographics (Vancouver, WA) and analyzed using a standard dissection and petrographic microscope equipped with cross-polarizers.

Clay content was determined based on grain size using the bouyoucous hydrometer test (ASTM D7928). Other chemical soil tests (K⁺, pH, Na⁺, Ca²⁺, Mg²⁺, and organic matter) were performed commercially by WARD Laboratories. Three samples were sent to the lab in duplicate to verify sampling and analytical repeatability (Supplemental Table S1). The sodium adsorption ratio (SAR) was calculated as (Brady and Weil 2008):

$$SAR = \frac{[Na^+]}{\sqrt{\frac{1}{2}([Ca^{2+}] + [Mg^{2+}])}}$$

Penetration resistance (soil surface strength)

The strength of the soil surface was evaluated using an automated Instron penetrometer (Rice and McEwan 2001; Rice et al. 1997), in which a blunt-end probe (6.9 mm diameter) affixed to a loading piston is pushed into the specimen at a constant rate of 1.3 mm/min, while the applied normal force and displacement are recorded continuously. Each specimen was tested multiple times, at least thrice, on visually undisturbed surfaces. The applied force (kiloNewtons) per unit area (square meter) has the units kiloPascals (kPa), which were plotted against the displacement (mm). The peak strength of the crust was determined as the average maximum stress (kPa) from the multiple runs.

We evaluated soil crust strength before and after inducing the formation of a surface crusts by wetting with deionized water and drying. We used ~150g of sieved soil (prepared as above) placed in a 100 mm diameter, 20 mm deep Petri dish. Background strength (CS_0) was evaluated using dry, sieved soil (not wetted).

Next, the same Petri dish was placed in a 110 cm x 50 cm x 70 cm terrarium provided with a Coospider Reptile Fogger, where a mist was applied until the surface of the soil maintained a visible sheen for more than 10 minutes, indicating the surficial soil had become nearly saturated. The soil was then dried under an AC Infinity S22 light on a 12-hour on-off cycle with a maximum intensity of $\sim 1000 \mu E m^{-2} sec^{-1}$, which created a peak temperature of $\sim 32^\circ C$, for at least two on-off cycles. After drying, the resistance to penetration was measured as above, yielding the fog-induced crust strength (CS_F).

Last, we simulated a rain-induced crust on the same specimen, by wetting to saturation with a PetraTools HD4000 garden sprayer, drying and measuring penetration resistance as above. This yielded the strength of a rain induced crust strength (CS_R).

Threshold velocity (dust generation potential)

A Portable In Situ Soil Wind Erosion Laboratory (PI-SWERL™ - Dust Quant LLC) was used to determine soil potential for dust formation by wind shear (Etyemezian et al. 2007). The PI-SWERL™ device (Supplemental Figure S1) is equipped with a rotating flat annular blade in a closed chamber positioned 6 cm above the soil surface. We used six progressive blade rotation speeds: 2000, 3000, 4000, 4500, 5000, and 6000 RPM, for 60 seconds each. Laser diffraction is used to measure the resulting particle emissions flux. Each rotor speed corresponds to a specific wind velocity. We report the wind velocity at which soil particles begin to detach, i.e. the threshold velocity (T_v). Soils were tested for particle emissions in the field and in the laboratory. Laboratory samples for PI-SWERL™ testing were prepared by lightly compacting 1.7-1.8 kg of surface soil into a 23 cm diameter x 2.5 cm pie pan and leveling off the surface to minimize surface roughness. The test was initially conducted on dried but untreated specimens and then repeated after creating an abiotic crust by rain-wetting and drying (as detailed for penetrometer testing).

Data analysis

To determine which chemical and/or physical properties influence abiotic crusting, we applied linear regression models using R, open source statistical analysis software (R-Core 2017). Correlations were performed on the increased fog-wetted crust strength ($\Delta CS_F = CS_F - CS_0$), increased rain-wetted crust strength ($\Delta CS_R = CS_R - CS_0$), and increased, or differential crust strength (DCS: $\Delta CS_R - \Delta CS_F$) versus each compositional variable. Once the (independent) linear model parameters were determined, we applied the Akaike algorithm (Akaike 2011) weight which model best described the data. As an alternative, we also considered and report

multi-variate models of regression, to determine if they would give a better fit. We considered using transformed data for percent clay content (Lin and Xu 2020), but this did not have a meaningful impact on overall results.

Results

Abiotic crust formation: potential and modes.

Abiotic soil crusting could be consistently replicated in the laboratory using a wet/dry treatment. Crust formation was evident by comparing the baseline soil strength (S_0) of untreated, sieved soil to that attained by fog-wetting and drying (CS_F). The magnitude of crusting determined by penetrometer varied considerably among samples, between 134 and 836 kPa (Table 1). A second round of crust formation, this time using simulated rainfall to include raindrop momentum in the crusting process (CS_R), resulted in penetration forces ranging from 153 to 1,562 kPa (Table 1). A single wet/dry cycle sufficed to form a crust, and additional wet/dry cycles did not result in increased strength regardless of watering mode (Supplemental Figure S2). In rain-wetted soils of sufficient clay content a thin surficial clay seal had formed, which was visible by a characteristic surface sheen when dry and patent in vertical petrographic thin sections (Figure 2), but such clay layers were absent in their fog-wetted counterparts. These observations are consistent with prior mechanistic notions of crust formation: dispersed clay platelets align as they dry, creating a depositional soil seal at the surface (Gillette et al. 1982; Laker and Nortjé 2019; Shainberg 1992). Generally, the net gain in strength of rain-induced crusts (ΔCS_R) was much higher than that of their corresponding fog induced crust (ΔCS_F), but in 3 out of 26 soils we found the opposite (Table 1). These soils, CG3(b), CG3(e) and Ros(a)] had very low clay content and did not form a clay layer.

Prior research (Vos et al. 2020) suggested that penetrometer crust strength may be useful in predicting the threshold velocity (T_v), a direct measure of dust generation potential by

wind shear. To confirm this relationship, we conducted both penetrometer and Tv determinations in a subset of our soil samples. Strength (ΔCS_R) indeed correlated with Tv (Figure 3; $R^2 = 0.72$, $p = 0.008$), predicting Tv with a slope of $4.6 \times 10^{-3} \pm 2.9 \times 10^{-3} \text{ m}^2 \text{ sec}^{-1} \text{ kPa}^{-1}$ (95% C.I.).

Compositional predictors of soil crusts strength

We evaluated the importance of compositional variables that could potentially predict CS_F and CS_R by applying a linear correlation model to each variable independently and report p values and slopes with the 95% confidence intervals (Table 2). For crust formed by fog watering, ΔCS_F was a strong direct function of carbonate content ($p < 0.0001$, Table 2, Figure 4a), which spanned a wide range of values from 0.2 to 20 % with a median value of 2.6 %. Carbonate content was in fact the best predictor among all variables measured. The usefulness of a predictive variable depends not only on the goodness of fit (R^2) to a linear model, but also on how far away from the slope is from zero. If the slope's 95% CI includes a zero value, the variable has no predictive usefulness. To represent this, we define the Predictive Usefulness Index (PUI) as the ratio of the minimal absolute slope value in the 95% CI range to the best fit slope. The PUI can range from 1 (best possible predictor) to 0 (useless as a predictor). Carbonate predicts ΔCS_F with a PUI of 0.55 (Table 2). While soil pH had a positive correlation with ΔCS_F ($p < 0.05$), it provided no predictive usefulness (PUI = 0; Table 2) because its slope 95% CI envelope included a slope of zero. Similarly, Mg^{2+} and Ca^{2+} were also correlated with ΔCS_F though only marginally significant ($p = 0.10$), and PUIs were 0.07 and 0 (Table 2). PUIs are consistent with an Akaike analysis of ΔCS_F : the weighted influence of carbonate was 99.79%. We also ran multivariate correlation analyses by combining all variables with carbonate against ΔCS_F , and again the model with carbonate alone gave the best fit (Supplemental Table S2). We conclude that ΔCS_F can only be predicted using carbonate content.

With respect to rain-induced crust strength (ΔCS_R), and considering only single variables, carbonate was also the best predictor of ΔCS_R ($p = 0.004$, Table 2), the one parameter with the highest Akaike weight (42%) and a PUI of 0.36 (Table 2, Figure 4b). Yet, the PUI for ΔCS_R carbonate (0.36) was lower than that for ΔCS_F carbonate (0.55). Other parameters (Ca^{2+} , Mg^{2+} , Na^+ , clay) had significant ($p < 0.05$) correlations but lower PUIs (Table 2). Mg^{2+} (PUI = 0.30) and to a lesser degree Na^+ (PUI = 0.20) appeared to be potentially useful as secondary predictors. A multiple regression analysis here shows that Carbonate + Clay (Supplemental S2; adjusted $R^2 = 0.40$) provided a better fit than carbonate alone ($R^2 = 0.30$) and had an Akaike weighted influence of 38%. Thus, while carbonate remains the main driver of ΔCS_R , the influence of clays on this parameter seems important as an additional mechanism to increase crust strength (Table 1). However, clay alone is not a useful predictor of ΔCS_R (PUI = 0.05, Table 2, Figure 4c).

To further test the notion that clay is important in rain-wetted crust strength, we investigated the relationships of the differential crust strength, $DCS = \Delta CS_R - \Delta CS_F$, with potential drivers. In this case, we saw the clay content had the strongest correlation ($p = 0.04$, Table 2, Figure 4d), where clay accounted for 27% of the Akaike weighted influence. This is consistent with our structural data in Figure 2. However, clay was not useful as a predictor (PUI = 0.07). The ions Ca^{2+} , Mg^{2+} and Na^+ seemed to contribute significantly ($p = 0.04$) to the increased strength in rain-induced crusts. However, because each cation had a high degree of co-correlation with clay (Ca^{2+} , $p < 0.001$; Mg^{2+} , $p = 0.002$; Na^+ , $p = 0.005$), any independent effect was likely masked. The multiple regression analysis for DCS also showed the importance of clay, even when clay + carbonate (adjusted $R^2 = 0.21$) gave a slightly better fit than clay alone ($R^2 = 0.17$; Supplemental Table S2). Thus, while clay appears to be the main driver of DCS, the contribution of carbonate to clay seal strength seems preeminent in terms of predictive value.

Discussion

We could show that carbonate content can be used as a predictor of abiotic crust formation and strength in farm soils from Pinal County in Arizona, and by deduction, to predict their potential as a source of wind-blown dust. Our experiments show that, following a soil-wetting event, drying causes carbonate (re)precipitation and soil cementation. This likely happens more prominently at the soil surface where water evaporation raises effective concentrations of carbonate and cations beyond their respective solubility products, promoting preferentially surface cementation, as a drop in water potential promotes upward flux of the soil solution to continuously feed the process. The current mechanistic framework for soil crust formation tends to emphasize clay re-deposition (Assouline 2004; Cattle et al. 2004) and downplays the role of cementation (McFadden et al. 1998; Robinson and Woodun 2008), but it has not proved useful as a predictive tool. We saw a very high degree of correlation (Table 2; $p < 0.0001$) between fog-wetted strength (CS_F) and carbonate, and a virtually exclusive dependence on this parameter. This conclusion is also supported indirectly by the positive relationship of pH to crust strength [S_F had a highly significant ($p < 0.05$, Table 2) correlation with pH], as an alkalinization increases the proportion of carbonate ion in the carbonate equilibrium, promoting precipitation, even within an invariant level of dissolved inorganic carbon (Stumm and Morgan 1996). This effect did not overwhelm the importance of the absolute carbonate content, and pH did not rise to the level of a good predictor. Similarly, divalent cation levels can be expected to correlate with crust strength, as they also influence how easily soil solution concentrations exceed the solubility product for carbonate minerals. Indeed, ΔCS_R had a high correlation with Mg^{2+} , and Ca^{2+} ($p < 0.03$, Table 2). We acknowledge that others have speculated on the role of carbonates in soil crusting (Feng et al. 2013; Gillette et al. 1982; Robinson and Woodun 2008; Virto et al. 2011), though without thorough experimental interrogations. By contrast, correlation between crust strength and clay content was weak. By

isolating the factors that cause deposition and cementation processes, our results not only point to a useful predictive tool but suggests an alternate explanation of the soil crusting mechanism in desert soils: abiotic crust strength in these environments is primarily controlled by carbonate precipitation, while clay sealing has a secondary effect that increases strength.

By comparing fog-wetted to rain-wetted soils, we were able to parse out cementation due to carbonate precipitation, eliminating raindrop energy as a factor needed to break apart and disperse aggregate-bound clays (McIntyre 1958). Comparisons of fog and rain-wetting used in the past have been applied to study infiltration rates, not crusting (Kaseke et al. 2012; Li et al. 2018), where rain-wetting decreases infiltration (Agassi et al. 1985). In these cases, the authors report how dispersed clays and sodium combine to create a water-resistant soil seal (Khatei et al. 2024), but cementation was not considered. And yet, consistent with the canonical mechanistic framework based on the formation of a depositional clay seal, DCS was most strongly correlated with clay ($p = 0.04$, Table 2). If clay sealing were the principal mechanism of increased crust strength, one should expect the content of Na^+ to be also important, because it acts as a clay dispersing agent (Parameswaran and Sivapullaiah 2017). Indeed, in our study Na^+ was also correlated with strength and is potentially a useful predictor of DCS (PUI = 0.42, Table 2).

A generalization of our conclusions beyond arid soils must be tempered by recognizing their uniqueness. Mechanistic studies have largely considered how the destructive force of raindrops destroy soil aggregates (Fan et al. 2008; Feng et al. 2013; McIntyre 1958), but this may not be applicable in our settings, as the our soils presented a low degree of aggregation, and we effectively removed small aggregates by sieving to mimic dry season plowing. These conditions may have dampened a larger effect of raindrop energy potentially present in non-agricultural soils. In addition, the aridisols we targeted may have enhanced the role of carbonate precipitation and cementation due their alkaline nature and high content of calcium, magnesium,

and carbonate ions (Dunkerley 2011). Processes that stabilize soil by increasing flocculation and aggregate formation (Singer and Warrington 1992) may not be as relevant in deserts.

While our study has implications for the mechanisms of desert soil crust formation, our primary objective was to find a predictive tool to estimate abiotic crust strength as a tool to aid in dust control measures. To that end, we have shown that carbonate is the best predictor of crust strength, a surrogate for dust forming potential (Rice et al. 1997) (and see Fig 3). While we obtained a favorable correlation of crust strength and T_v for dust formation ($p = 0.008$, Figure 3), we acknowledge limitations of our findings. PI-SWERL™ results require expertise to interpret (Supplemental Figure S3), and penetrometer tests can be variable, with the potential for false positives and outliers (Supplemental Figure S4). In addition, we extended our dust susceptibility prediction across two correlative steps (carbonate to CS_R and on to dust formation potential).

We contend that fugitive dust control in large areas such as Pinal County can be optimized by identification of soils with weak crusting potential, and prioritizing interventions there. In this regard the soil's carbonate content constitutes a suitable screening parameter that is measurable with simple, portable tests. Some carbonate content data is immediately available in public databases, such as the USGS Soil Survey, although local carbonate testing would be prudent, since soils within a single type can be variable in carbonate content and dust susceptibility (for example, consider the CG3 series in Table 1). It is possible to map the estimated wind erodibility of soils based on carbonate content. We provide an example in Supplemental Figure S5. Previous work on modeling aeolian dust concentrations in Pinal County using soil texture met with limited success (Joshi 2021), and our work suggests that inclusion of carbonate content may lead to improvements. We note here that such a model would only predict dust potential from undisturbed soils because continual disturbance by plowing effectively destroys the soil armor. Based on our lab and field observations, all

disturbed soils are potential dust sources, so both soil stabilization and modified farming practices in fallow fields are required for effective dust mitigation strategies.

Acknowledgements

Paco Ollerton help us navigate within the Pinal County farming community, and, as a member of the ADEQ Agricultural PM10 Best Management Practices Committee for dust control, providing insight into existing dust control efforts. Dr. Xi Yu performed some of the lab testing and analysis and Dr. Pierre Herckes provided helpful editorial comments.

Author Contribution statement

BS and FGP prepared the manuscript, with sections contributed by ES. FGP directed the research. EK and ES directed the penetrometer and PI-SWERLTM testing and, along with MF, provided manuscript edits. SAA and AHA performed the penetrometer and PI-SWERLTM testing. JLZ coordinated soil thin section mounts and accompanying microscopy.

Financial Support

Funding for this research was provided by a grant from the Arizona Board of Regents (#31)

Conflict of Interest statement

Conflicts of Interest: None

Ethics statements (if appropriate)

Data Availability statement

All results are listed in Tables 1 and S1.

References

- Agassi M, Morin J and Shainberg I** (1985) Effect of Raindrop Impact Energy and Water Salinity on Infiltration Rates of Sodic Soils. *SSSAJ* **49**, 186-190.
- Akaike H** (2011) Akaike's information criterion. *International encyclopedia of statistical science*, 25.
- Assouline S** (2004) Rainfall-Induced Soil Surface Sealing: A Critical Review of Observations, Conceptual Models, and Solutions. *VADOSE ZONE J.* **3**.
- Awadhwal NK and Thierstein GE** (1985) Soil crust and its impact on crop establishment: A review. *Soil and Tillage Research* **5**(3), 289-302. [https://doi.org/10.1016/0167-1987\(85\)90021-2](https://doi.org/10.1016/0167-1987(85)90021-2).
- Belnap J and Gillette DA** (1997) Disturbance of biological soil crusts: impacts on potential wind erodibility of sandy desert soils in southeastern Utah. *Land Degradation & Development* **8**(4), 355-362. [https://doi.org/10.1002/\(SICI\)1099-145X\(199712\)8:4<355::AID-LDR266>3.0.CO;2-H](https://doi.org/10.1002/(SICI)1099-145X(199712)8:4<355::AID-LDR266>3.0.CO;2-H).
- Brady NC and Weil RR** (2008) *The nature and properties of soils*, Rev. 14th edn. Upper Saddle River, N.J. ;: Pearson Prentice Hall.
- Bungartz F, Garvie LAJ and Nash TH** (2004) Anatomy of the endolithic Sonoran Desert lichen *Verrucaria rubrocincta* Breuss: implications for biodeterioration and biomineralization. *The Lichenologist* **36**(1), 55-73. <https://doi.org/10.1017/s0024282904013854>.
- Cattle S, Cousin I, Darboux F and Bissonnais YL** (2004) The effect of soil crust ageing, through wetting and drying, on some surface structural properties.
- Dunkerley DL** (2011) Desert Soils. In Thomas DSG (ed), *Arid Zone Geomorphology*. 1 ed.: Wiley, 101-129.
- Etyemezian V, Nikolich G, Ahonen S, Pitchford M, Sweeney M, Purcell R, Gillies J and Kuhns H** (2007) The Portable In Situ Wind Erosion Laboratory (PI-SWERL): A new method to measure PM10 windblown dust properties and potential for emissions. *Atmospheric Environment* **41**(18), 3789-3796. <https://doi.org/10.1016/j.atmosenv.2007.01.018>.
- Fan Y, Lei T, Shainberg I and Cai Q** (2008) Wetting Rate and Rain Depth Effects on Crust Strength and Micromorphology. *Soil Science Society of America Journal* **72**(6), 1604-1610. <https://doi.org/10.2136/sssaj2007.0334>.
- Feng G, Sharratt B and Vaddella V** (2013) Windblown soil crust formation under light rainfall in a semiarid region. *Soil and Tillage Research* **128**, 91-96. <https://doi.org/10.1016/j.still.2012.11.004>.
- Finn DR, Maldonado J, de Martini F, Yu J, Penton CR, Fontenele RS, Schmidlin K, Kraberger S, Varsani A, Gile GH, Barker B, Kollath DR, Muenich RL, Herckes P, Fraser M and Garcia-Pichel F** (2021) Agricultural practices drive biological loads, seasonal patterns and potential pathogens in the aerobiome of a mixed-land-use dryland. *Science of The Total Environment* **798**, 149239. <https://doi.org/10.1016/j.scitotenv.2021.149239>.
- Forster S and Goldberg HS** (1990) Flocculation of Reference Clays and Arid-Zone Soil Clays. *Soil Science Society of America Journal* **54**, 714-718.
- Gillette DA, Adams J, Muhs D and Kihl R** (1982) Threshold friction velocities and rupture moduli for crusted desert soils for the input of soil particles into the air. *Journal of Geophysical Research* **87**(C11), 9003. <https://doi.org/10.1029/JC087iC11p09003>.
- Ginoux P, Prospero JM, Gill TE, Hsu NC and Zhao M** (2012) Global-scale attribution of anthropogenic and natural dust sources and their emission rates based on MODIS Deep Blue aerosol products: ANTHROPOGENIC AND NATURAL DUST SOURCES. *Reviews of Geophysics* **50**(3). <https://doi.org/10.1029/2012RG000388>.

- Hamdan N and Kavazanjian E** (2016) Enzyme-induced carbonate mineral precipitation for fugitive dust control. *Géotechnique* **66**(7), 546-555.
<https://doi.org/10.1680/jgeot.15.P.168>.
- Henry MB, Mozer M, Rogich JJ, Farrell K, Sachs JW, Selzer J, Chikani V, Bradley G and Comp G** (2023) Haboob Dust Storms and Motor Vehicle Collision-related Trauma in Phoenix, Arizona. *Western Journal of Emergency Medicine* **24**(4).
<https://doi.org/10.5811/WESTJEM.59381>.
- Heredia-Velásquez AM, Giraldo-Silva A, Nelson C, Bethany J, Kut P, González-de-Salceda L and Garcia-Pichel F** (2023) Dual use of solar power plants as biocrust nurseries for large-scale arid soil restoration. *Nature Sustainability* **6**(8), 955-964.
<https://doi.org/10.1038/s41893-023-01106-8>.
- Huang J, Li Y, Fu C, Chen F, Fu Q, Dai A, Shinoda M, Ma Z, Guo W, Li Z, Zhang L, Liu Y, Yu H, He Y, Xie Y, Guan X, Ji M, Lin L, Wang S, Yan H and Wang G** (2017) Dryland climate change: Recent progress and challenges. *Reviews of Geophysics* **55**(3), 719-778. <https://doi.org/10.1002/2016rg000550>.
- Jalilian J, Moghaddam SS and Tagizadeh Y** (2017) Accelerating Soil Moisture Determination with Microwave Oven. *Journal of Chinese Soil and Water Conservation* **48**(2), 101-103.
- Joshi JR** (2021) Quantifying the impact of cropland wind erosion on air quality: A high-resolution modeling case study of an Arizona dust storm. *Atmospheric Environment* **263**, 118658. <https://doi.org/10.1016/j.atmosenv.2021.118658>.
- Kaseke KF, Mills AJ, Esler K, Henschel J, Seely MK and Brown R** (2012) Spatial Variation of “Non-Rainfall” Water Input and the Effect of Mechanical Soil Crusts on Input and Evaporation. *Pure and Applied Geophysics* **169**(12), 2217-2229.
<https://doi.org/10.1007/s00024-012-0469-5>.
- Khatei G, Rinaldo T, Van Pelt RS, D’Odorico P and Ravi S** (2024) Wind Erodibility and Particulate Matter Emissions of Salt-Affected Soils: The Case of Dry Soils in a Low Humidity Atmosphere. *Journal of Geophysical Research: Atmospheres* **129**(1).
<https://doi.org/10.1029/2023jd039576>.
- Laker MC and Nortjé GP** (2019) Review of existing knowledge on soil crusting in South Africa. In *Advances in Agronomy*. Elsevier, 189-242.
- Li J, Kandakji T, Lee JA, Tatarko J, Blackwell J, Gill TE and Collins JD** (2018) Blowing dust and highway safety in the southwestern United States: Characteristics of dust emission “hotspots” and management implications. *Science of The Total Environment* **621**, 1023-1032. <https://doi.org/10.1016/j.scitotenv.2017.10.124>.
- Lin L and Xu C** (2020) Arcsine-based transformations for meta-analysis of proportions: Pros, cons, and alternatives. *Health Science Reports* **3**(3), e178.
<https://doi.org/10.1002/hsr2.178>.
- McFadden LD, McDonald EV, Wells SG, Anderson K, Quade J and Forman SL** (1998) The vesicular layer and carbonate collars of desert soils and pavements: formation, age and relation to climate change. *Geomorphology* **24**(2-3), 101-145.
[https://doi.org/10.1016/S0169-555X\(97\)00095-0](https://doi.org/10.1016/S0169-555X(97)00095-0).
- McIntyre DS** (1958) Permeability measurements of soil crusts formed by raindrop impact. *Soil science* **85**(4), 185-189.
- Oswal MC** (1994) Water Conservation and Dryland Crop Production in Arid and Semi-Arid Regions. *Annals of Arid Zone* **33**(2), 95-104.
- Parameswaran TG and Sivapullaiah PV** (2017) Influence of Sodium and Lithium Monovalent Cations on Dispersivity of Clay Soil. *Journal of Materials in Civil Engineering* **29**(7).
[https://doi.org/10.1061/\(ASCE\)MT.1943-5533.000187](https://doi.org/10.1061/(ASCE)MT.1943-5533.000187).
- Piemeisel RL, Lawson FR and Carsner E** (1951) Weeds, Insects, Plant Diseases, and Dust Storms. *Science* **73**(2).

- R-Core T** (2017) A language and environment for statistical computing. In.: R Foundation for Statistical Computing, Vienna, Austria.
- Ramakrishnan B, Lueders T, Dun PF and Friedrich MW** (2001) Archaeal community structures in rice soils from different geographical regions before and after initiation of methane production. *FEMS Microbiology Ecology* **37**, 12.
- Rice MA and McEwan IK** (2001) Crust strength: a wind tunnel study of the effect of impact by saltating particles on cohesive soil surfaces. *Earth Surface Processes and Landforms* **26**(7), 721-733. <https://doi.org/10.1002/esp.217>.
- Rice MA, Mullins CE and McEwan IK** (1997) An analysis of soil crust strength in relation to potential abrasion by saltating particles. *Earth Surface Processes and Landforms* **22**(9), 869-883. [https://doi.org/10.1002/\(SICI\)1096-9837\(199709\)22:9<869::AID-ESP785>3.0.CO;2-P](https://doi.org/10.1002/(SICI)1096-9837(199709)22:9<869::AID-ESP785>3.0.CO;2-P).
- Rice MA, Willetts BB and McEwan IK** (1996) Wind Erosion of Crusted Sediement Soils. *Earth Surface Processes and Landforms* **21**(3), 279-293. [https://doi.org/10.1002/\(SICI\)1096-9837\(199603\)21:3<279::AID-ESP633>3.0.CO;2-A](https://doi.org/10.1002/(SICI)1096-9837(199603)21:3<279::AID-ESP633>3.0.CO;2-A).
- Robinson DA and Woodun JK** (2008) An experimental study of crust development on chalk downland soils and their impact on runoff and erosion. *European Journal of Soil Science* **59**(4), 784-798. <https://doi.org/10.1111/j.1365-2389.2008.01033.x>.
- Shainberg I** (1992) Chemical and Mineralogical Components of Crusting. In Summer ME and Stewart BA (eds), *Soil crusting: chemical and physical processes*. Boca Raton, FL: Soil crusting: chemical and physical processes.
- Singer MJ and Warrington DN** (1992) Crusting in the Western United States. In Summer ME and Stewart BA (eds), *Soil crusting: chemical and physical processes*. Boca Raton, FL: Soil crusting: chemical and physical processes.
- Stovall MS, Ganguli AC, Schallner JW, Faist AM, Yu Q and Pietrasiak N** (2022) Can biological soil crusts be prominent landscape components in rangelands? A case study from New Mexico, USA. *Geoderma* **410**, 115658. <https://doi.org/10.1016/j.geoderma.2021.115658>.
- Stumm W and Morgan JJ** (1996) *Aquatic Chemistry. Chemical Equilibria and Rates in Natural Waters*, 3rd edn.: John Wiley & Sons, Inc.
- Tibke G** (1988) Basic Principles of Wind Erosion Control. *Agriculture, Ecosystems and Environment* **22/23**, 103-122.
- Tippkötter R and Ritz K** (1996) Evaluation of polyester, epoxy and acrylic resins for suitability in preparation of soil thin sections for in situ biological studies. *Geoderma* **69**(1), 31-57. [https://doi.org/https://doi.org/10.1016/0016-7061\(95\)00041-0](https://doi.org/https://doi.org/10.1016/0016-7061(95)00041-0).
- Vergadi E, Rouva G, Angeli M and Galanakis E** (2022) Infectious Diseases Associated with Desert Dust Outbreaks: A Systematic Review. *International Journal of Environmental Research and Public Health* **19**(11), 6907. <https://doi.org/10.3390/ijerph19116907>.
- Virto I, Gartzia-Bengoetxea N and Fernández-Ugalde O** (2011) Role of Organic Matter and Carbonates in Soil Aggregation Estimated Using Laser Diffractometry. *Pedosphere* **21**(5), 566-572. [https://doi.org/10.1016/S1002-0160\(11\)60158-6](https://doi.org/10.1016/S1002-0160(11)60158-6).
- Vos H, Fister W, Eckardt F, Palmer A and Kuhn N** (2020) Physical Crust Formation on Sandy Soils and Their Potential to Reduce Dust Emissions from Croplands. *Land* **9**(12), 503. <https://doi.org/10.3390/land9120503>.
- Vos HC, Karst IG, Eckardt FD, Fister W and Kuhn NJ** (2022) Influence of Crop and Land Management on Wind Erosion from Sandy Soils in Dryland Agriculture. *Agronomy* **12**(2), 457. <https://doi.org/10.3390/agronomy12020457>.
- Williams AJ, Pagliai M and Stoops G** (2018) Physical and Biological Surface Crusts and Seals. In *Interpretation of Micromorphological Features of Soils and Regoliths*. 539-574.

Tables and Figure Captions

Table 1 – **Soil designations, physical, textural and chemical properties of soil samples in our survey.** CS₀ = Crust Strength of dry, sieved soil measured as penetration resistance in kiloPascals (kPa). CS_F = Crust Strength after wetting soil with Fog. CS_R = Crust Strength after wetting soil with simulated Rain. Δ CS_F = Increase in Crust Strength due to Fog (CS_F – CS₀). Δ CS_R = Increase in Crust Strength due to simulated Rain (CS_R – CS₀). DCS = Differential Crust Strength due to simulated Rain compared to Fog (Δ CS_R - Δ CS_F). Na⁺ = Sodium, Ca²⁺ = Calcium, Mg²⁺ = Magnesium, SAR = Sodium Absorption Ratio, OM = Organic Matter, K⁺ = Potassium. Shading separates soil types with the same series name.

Soil	Crust Strength (kPa)						Textural and Chemical Soil Properties								
	Measured values			Derived Values			Measured values								Calculated
	CS ₀	CS _F	CS _R	Δ CS _F	Δ CS _R	DCS	Carbonate (%)	Clay (%)	pH	Na ⁺ (ppm)	Ca ²⁺ (ppm)	Mg ²⁺ (ppm)	OM (%)	K ⁺ (ppm)	SAR
CG3(a)	4.9	134.2	373.8	129.3	368.9	239.6	0.52	8.7	8.0	46	1,768	220	1.7	442	1.46
CG3(b)	8.1	306.8	172.7	298.7	164.6	-134.1	0.46	3.8	8.3	17	1,765	193	0.6	310	0.54
CG3(c)	18.8	430.3	1,069	411.5	1,050	638.8	4.62	16.6	8.2	265	4,339	454	1.6	704	5.41
CG3(d)	18.4	319.9	479.5	301.5	461.1	159.6	1.20	4.4	9.0	112	2,894	166	0.6	400	2.86
CG3(e)	14.7	520.7	384.7	506.0	370.0	-136.0	8.07	6.3	8.5	123	3,519	282	1.6	970	2.82
CG3(f)	17.7	330.5	518.8	312.8	501.1	188.3	0.47	6.3	8.3	37	1,578	180	0.7	375	1.25
CG4(a)	27.2	494.2	652.4	467.0	625.2	158.2	5.50	17.1	8.2	115	4,890	467	2.5	1048	2.22
Con(a)	16.9	504.9	806.9	488.0	790.0	302.0	0.21	9.4	7.7	38	1,084	359	1.1	633	1.41
Gil(a)	4.5	216.8	468.5	212.3	464.0	251.7	2.32	11.3	8.4	195	3,198	366	1.5	967	4.62
Gil(b)	3.3	411.4	828.5	408.1	825.2	417.1	3.01	7.6	8.3	202	3,661	383	1.8	400	4.49
Gin(a)	5.9	597.1	1,110	591.2	1,104	512.5	2.58	21.9	8.5	521	5,467	307	2.2	572	9.70
Gla(a)	5.2	306.7	758.3	301.5	753.1	451.6	2.27	25.0	8.4	165	6,446	283	2.2	744	2.84
Gle(a)	8.1	374.7	533.4	366.6	525.3	158.7	2.07	25.0	8.4	35	6,676	282	2.1	673	0.59
Gle(b)	9.9	525.5	1,526	515.6	1,516	1,001	3.76	29.8	8.1	423	5,827	567	2.5	1,010	7.48
LaP(a)	7.4	836.3	1,561	828.9	1,554	724.6	15.22	16.4	8.8	109	3,902	362	1.3	468	2.36
LaP(b)	1.2	733.8	1,562	732.6	1,561	828.0	19.47	9.4	8.6	221	4,225	428	2.4	475	4.58
Lav(a)	11.4	556.5	1,007	545.1	995.1	450.0	10.17	7.6	8.7	192	3,850	311	1.6	860	4.21
Mar(a)	13.2	257.5	459.5	244.3	446.3	202.0	1.12	8.8	8.1	18	3,103	246	0.9	353	0.44
Mar(b)	15.8	513.3	1,065	497.5	1,049	551.5	4.92	9.0	8.7	192	5,548	288	1.9	733	3.55
Mes(a)	9.2	291.0	1,129	281.8	1,120	837.7	1.49	8.8	8.3	46	3,099	296	2.0	538	1.12
Moh(a)	11.0	312.5	1,246	301.5	1,235	933.0	2.66	11.9	8.6	113	3,815	292	1.1	712	2.49
Ros(a)	8.8	163.3	153.0	154.5	144.2	-10.3	0.17	3.8	8.2	6	1,355	97	0.4	158	0.22
Tol(a)	10.3	266.5	1,031	256.2	1,020	764.0	5.59	10.0	8.6	73	3,767	161	0.8	932	1.65
Tol(b)	13.6	706.7	1,130	693.1	1,116	423.2	5.19	10.0	8.3	180	3,702	207	1.1	1,075	4.07
Tol(c)	12.5	258.0	377.1	245.5	364.6	119.1	9.54	10.2	8.1	280	4,247	353	1.8	497	5.84
Tri(a)	7.7	160.0	622.0	152.3	614.3	462.0	1.95	17.1	8.4	250	3,755	326	2.2	867	5.53

Table 2 – Correlation of soil crust strength parameters with single primary predictive variables. Soil crust strength measures are: ΔCS_F = Fog-wetted strength. ΔCS_R = Rain-wetted strength, and ΔCS = Differential Crust Strength (Rain – Fog). Among variables, SAR = Sodium Absorption Ratio, and OM for Organic Matter. Listed statistics are Pearson coefficient (Pearson) for a linear model, the probability that there is no correlation (p), the goodness of linear fit (R^2), and the best-fit slope (slope), representing the change in strength divided by the change in the explanatory variable value, with its 95% confidence interval. Slope units vary: Carbonate + Clay = KPa / (g / 100 g soil); cations & OM = KPa / (g / 1×10^6 g soil); pH + SAR = KPa / (unitless). PUI stands for Predictive Usefulness Index, which is calculated as the ratio of the minimal absolute slope value in the 95% CI range to the best fit slope and varies from 1 (best possible predictor) to 0 (useless as a predictor). Akaike weights depict the cumulative contribution of each additional variable to the percent of variation predicted by the primary variable (bolded) in order of decreasing contributions.

	PEARSON	P	R ²	SLOPE	PUI	AKAIKE % (SINGLE VARIABLE)
Fog (ΔCS_F)						
Carbonate	0.69	<0.0001	0.48	26.6 ± 11.9	0.55	0.9979
pH	0.37	< 0.05	0.14	192 ± 268	0	0.9985
Ca ²⁺	0.31	0.10	0.10	0.040 ± 0.049	0	0.9988
Mg ²⁺	0.31	0.10	0.10	0.71 ± 0.66	0.07	0.9992
Na ⁺	0.29	0.13	0.08	0.51 ± 0.58	0	0.9994
SAR	0.28	0.15	0.08	26.4 ± 31.4	0	0.9997
OM	0.21	0.28	0.04	78 ± 117	0	0.9998
Clay	0.13	0.52	0.02	5.5 ± 10.9	0	0.9999
K ⁺	0.13	0.50	0.02	0.17 ± 0.29	0	1.0000
Rain (ΔCS_R)						
Carbonate	0.55	0.004	0.3	48.1 ± 31.0	0.36	0.42
Mg ²⁺	0.46	0.006	0.27	2.0 ± 1.4	0.30	0.69
Na ⁺	0.29	0.02	0.21	1.5 ± 1.2	0.20	0.78
Ca ²⁺	0.43	0.03	0.19	0.12 ± 0.11	0.08	0.84
SAR	0.43	0.03	0.18	76.9 ± 68.2	0.11	0.89
Clay	0.41	0.04	0.16	24.2 ± 23.1	0.05	0.93
OM	0.40	0.05	0.16	259 ± 254	0.02	0.97
K ⁺	0.31	0.13	0.09	0.50 ± 0.65	0	0.99
pH	0.29	0.15	0.09	442 ± 606	0	1.00
Rain – Fog (DCS)						
Clay	0.41	0.04	0.17	18.8 ± 17.4	0.07	0.27
Ca ²⁺	0.39	0.04	0.15	0.08 ± 0.08	0	0.42
Na ⁺	0.39	0.04	0.15	1.0 ± 0.58	0.42	0.56
Mg ²⁺	0.39	0.04	0.15	1.33 ± 1.11	0.17	0.70
SAR	0.35	0.06	0.12	50.5 ± 53.2	0	0.79
Carbonate	0.32	0.09	0.11	21.5 ± 26.6	0	0.86

Accepted Manuscript

OM	0.32	0.09	0.10	181 ± 195	0	0.92
K ⁺	0.30	0.12	0.09	0.32 ± 0.50	0	0.97
pH	0.29	0.23	0.05	250 ± 470	0	1.00

Figure 1 – **Soil sample locations used for this study.** All location are within Pinal County, Arizona. Summer monsoons, the primary source of dust storms, often travel northward through Pinal County into metropolitan Phoenix.

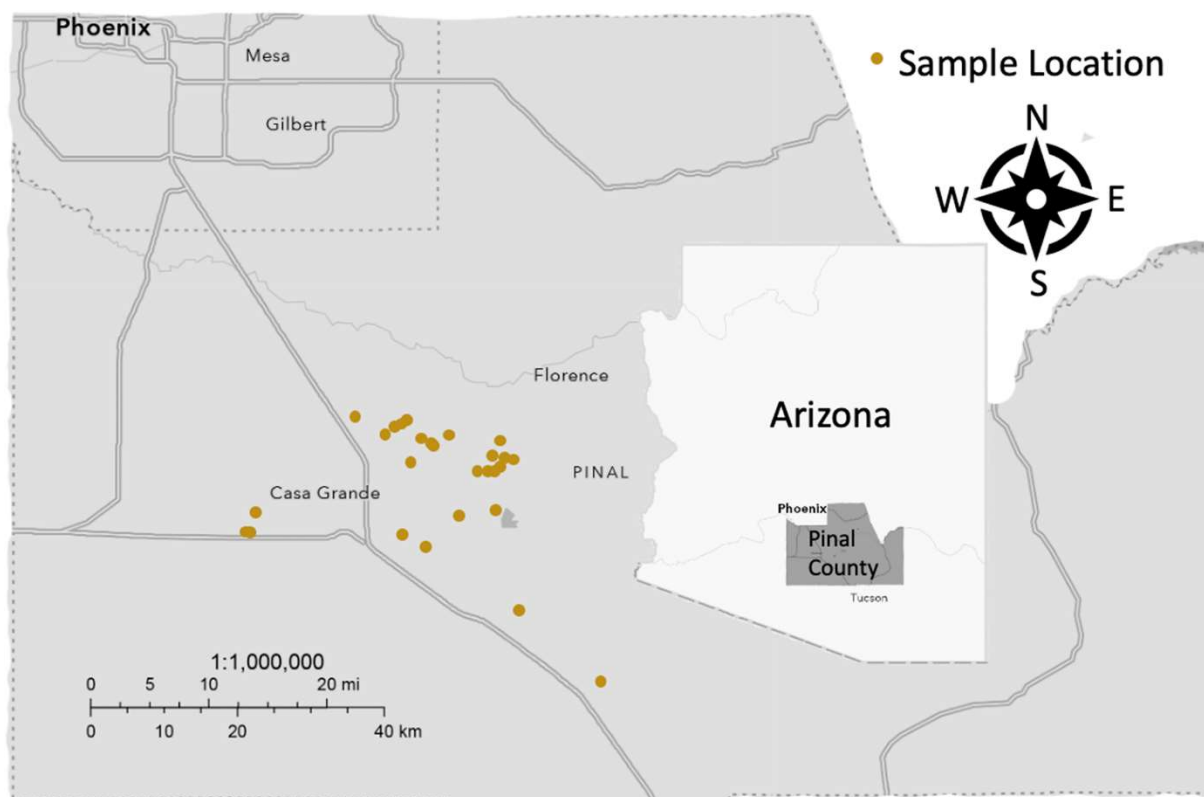


Figure 2. **Geological thin section photomicrographs of Tol(a) soil, a recently fallowed farm plot.** a) Soil collected from an area that had recently been plowed (prior to any subsequent rain events) showing a lack of developed soil crust. b) Soil collected from the same area after winter rains had created a thin seal layer (red arrows).

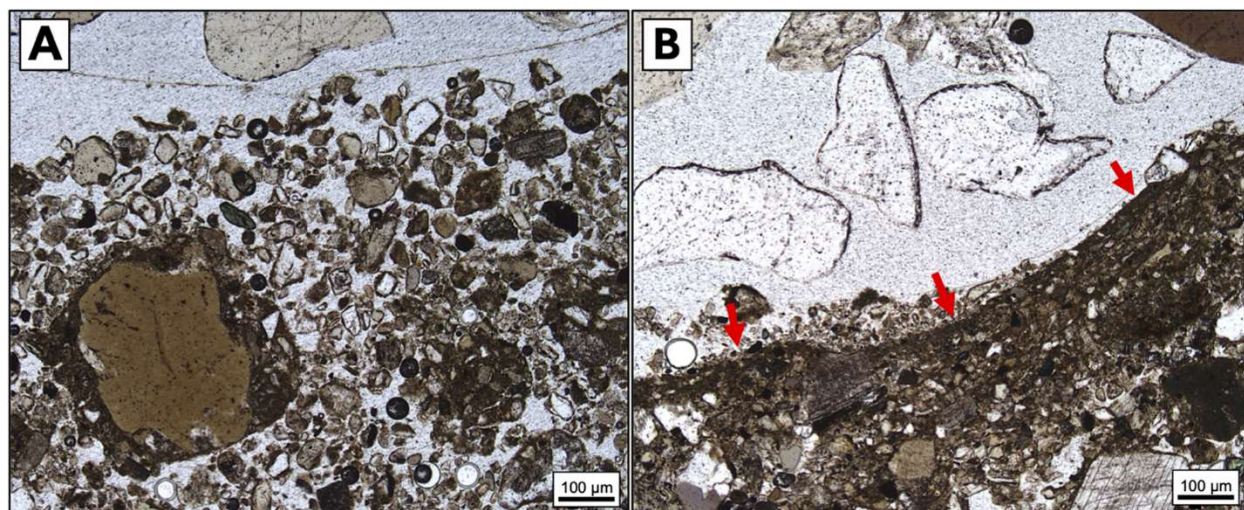


Figure 3. **Correlation of PI-SWERL[®]-determined Threshold Velocity (T_v) with penetrometer-measured Rain-Wetted Crust Strength (ΔCS_R).** Solid line represents best-fit linear regression, with 95% confidence intervals (shaded area). $n = 8$, PCC = Pearson Correlation Coefficient, kPa = kiloPascals

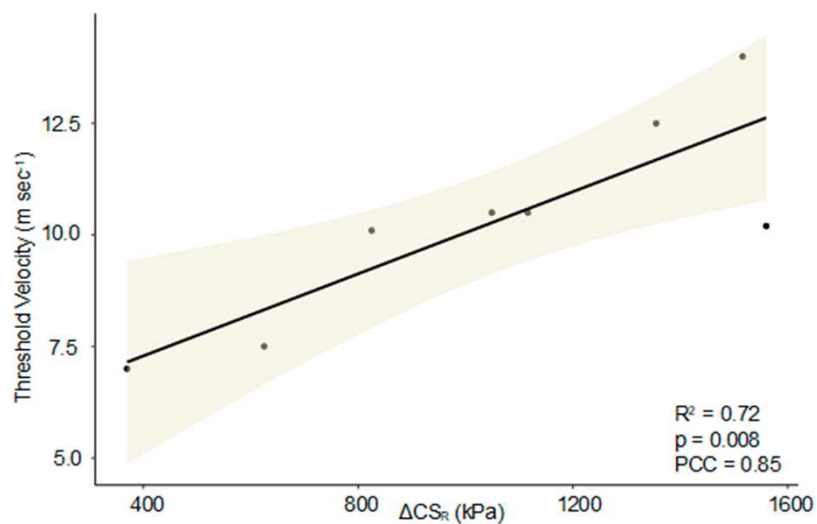


Figure 4. **Best-fit models for abiotic crust strength as a function of predictive variables.** PCC = Pearson Correlation Coefficient, kPa = kiloPascals. Solid line represents the best-fit linear model. The shaded area shows the 95% Confidence Interval for the slope ($n = 26$). The dashed line in (c) shows that the range includes a slope of 0 (Predictive Usefulness Index (PUI) = 0) and therefore is useless as a predictor. The comparable dashed line in (d) has a very small positive slope (PUI = 0.07) and therefore has minimal usefulness as a predictor.

